J Biomol NMR (2009) 43:187–196
DOI 10.1007/s10858-009-9302-6

ARTICLE

Relaxation-optimised Hartmann–Hahn transfer using a specifically Tailored MOCCA-XY16 mixing sequence for carbonyl–carbonyl correlation spectroscopy in ^{13}C direct detection NMR experiments

Isabella C. Felli · Roberta Pierattelli · Steffen J. Glaser · Burkhard Luy

Received: 7 November 2008 / Accepted: 6 January 2009 / Published online: 18 February 2009

Abstract Isotropic mixing sequences are one of the key methods to achieve efficient coherence transfer. Among them, the MOCCA-XY16, which keeps the magnetization longitudinal for a significant amount of time, is characterised by favourable relaxation properties. We show here that its adapted version is particularly suited for carbonyl–carbonyl correlations in ^{13}C direct detection NMR experiments.

Keywords NMR · Isotropic mixing · Protein NMR · ^{13}C detection · *Protonless* · Sequence specific assignment

Introduction

Routinely used in organic chemistry and in pharmaceutical chemistry to study small molecules (Breitmaier et al. 1970), ^{13}C direct detection NMR experiments provide very useful information on their structure and dynamics. Proposed in the 1980s also to study large biological macromolecules (Oh et al. 1988), ^{13}C direct detection NMR experiments were left behind for inverse detection methods, in which ^{13}C spins are studied in the indirect dimension of ^{1}H direct detection NMR experiments, due to the intrinsic higher sensitivity of ^{1}H compared to that of ^{13}C. The recent, tremendous improvements in instrumental sensitivity obtained with the increase in the available magnetic field strength and the advent of cryogenically cooled probeheads (Kovacs et al. 2005), mainly exploited to study systems with limited solubility through ^{1}H direct detection NMR experiments, can also be used to perform direct detection of low-γ nuclei for biomolecular NMR. Stimulated by this new perspective, a series of *exclusively heteronuclear* NMR experiments based on ^{13}C direct detection (*protonless* NMR) have been developed that enable complete sequence specific assignment of a protein without actively exploiting protons (Bermel et al. 2005a, b, 2006a, c; Bertini et al. 2004a). These experiments can be used as a complementary tool to proton detected NMR experiments for biomolecular applications, providing independent information always welcome on complex systems or for automatic-assignment purposes. The *protonless* NMR experiments are, however, essential to study specific systems where ^{1}H direct detection experiments are bound to fail, such as paramagnetic systems (Kolczak et al. 1999; Bertini et al. 2001; Machonkin et al. 2002; Kostic et al. 2002; Bermel et al. 2003; Arnesano et al. 2003; Babini et al. 2004; Caillet-Saguy et al. 2006; Bertini et al. 2007), where the line broadening experienced by ^{1}H is at least an order of magnitude larger than that experienced by ^{13}C, or very large systems for which ^{2}H labelling is often necessary to reduce ^{13}C linewidths (Eletsky et al. 2003; Bertini et al. 2004b, c; Vögeli et al. 2004; Matzapetakis et al. 2007; Bermel et al. 2007). For reasons other than fast transverse relaxation, ^{13}C direct detection NMR experiments, in particular those based on carbonyl direct detection, are very useful to study unfolded systems where C′ and N^{H} nuclei retain the largest chemical shift dispersion upon loss of a stable 3D structure (Bermel et al. 2006b). When transverse relaxation is not the limiting factor, the experiments based on ^{13}C direct detection may

I. C. Felli · R. Pierattelli
Department of Chemistry and Magnetic Resonance Center (CERM), University of Florence, Via Luigi Sacconi 6, 50019 Sesto Fiorentino, Florence, Italy

S. J. Glaser · B. Luy (✉)
Department of Chemistry, Technische Universität München, Lichtenbergstr. 4, 85747 Garching, Germany
e-mail: Burkhard.Luy@ch.tum.de

also benefit from the use of proton polarization as a starting point (^{1}H-start) and several experiments have been proposed both for proteins and nucleic acids (Fiala and Sklenar 2007; Farès et al. 2007; Hu et al. 2007; Bermel et al. accepted).

One of the widely used approaches to achieve coherence transfer and detect internuclear correlations is based on isotropic mixing sequences (Braunschweiler and Ernst 1983; Glaser and Quant 1996). These are particularly efficient in ^{13}C spin systems where either large one bond scalar couplings or smaller two or three bond scalar couplings can be exploited to achieve coherence transfer for different kinds of applications. However, efficient transverse relaxation can become one of the limiting factors for practical applications and the MOCCA-XY16 multiple pulse sequence (Kramer et al. 2001; Furrer et al. 2004) provides excellent performance by minimizing transverse relaxation contributions during the mixing time. On these grounds incorporation of the MOCCA-XY16 in different kinds of *protonless* NMR experiments is thus highly desirable.

Here we address the problem of isotropic mixing between spins for carbonyl–carbonyl transfer mediated by the small ^3J carbonyl–carbonyl scalar couplings to detect sequential correlations between carbonyls in proteins. The exploitation of ^3J carbonyl–carbonyl scalar coupling, proposed earlier either to achieve sequential correlations or structural information on the relevant dihedral angle (Grzesiek and Bax 1997; Liu et al. 2000), has recently been implemented in ^{13}C direct detection NMR experiments (Bermel et al. 2006b; Balayssac et al. 2006). The COCON experiment, in particular, proved very efficient in providing, in combination with one other 3D carbonyl detected experiment, the information to achieve complete sequence specific assignment of the backbone heteronuclei and of the C^β nuclei in α-synuclein, a 14.4 kDa natively unfolded protein (Bermel et al. 2006b). We compare here the relative performance of the isotropic mixing sequence previously used (FLOPSY-16 (Kadkhodaie et al. 1991)) with an adapted MOCCA-XY16 isotropic mixing scheme (Furrer et al. 2004) to achieve carbonyl–carbonyl transfer. In order to achieve best possible transfer properties, the parameters of the MOCCA-XY16 have been specifically optimised to the desired needs, i.e. efficient decoupling of C^α carbons and delays matched for maximum signal intensities.

Materials and methods

^{13}C, ^{15}N labelled ubiquitin sample was purchased from ProtEra srl (Sesto Fiorentino, Italy) and used without further manipulations. The protein concentration was 0.5 mM in 50 mM phosphate buffer, pH 7, 0.02% NaN_3.

All NMR experiments were performed at 16.4 T on a Bruker Avance spectrometer operating at 700.06 ^{1}H and 176.03 ^{13}C frequencies, equipped with a ^{13}C cryogenically cooled probehead optimised for ^{13}C direct detection.

The following parameters were employed. The ^{1}H, ^{13}C and ^{15}N carrier frequencies were placed at 7.0, 57.8 and 118.0 ppm, respectively, and ^{13}C pulses were given at 176.8 and 57.8 ppm to excite or invert C′ and C^α spins, respectively. Composite pulse decoupling was applied during acquisition and during some of the elements of the pulse sequence with RF field strengths of 1.6 kHz and 1.0 kHz for ^{1}H [WALTZ-16 (Shaka et al. 1983)] and ^{15}N [GARP-4 (Shaka et al. 1985)], respectively. For ^{13}C the following pulses were used: 320 μs with Q5 (and time reversed Q5) shapes (Emsley and Bodenhausen 1990) for C^α, C^{ali} excitation, 330 μs Q3 shape for C′ or C^α inversion and an adiabatic pulse [smoothed CHIRP (Boehlen and Bodenhausen 1993)] of 500 μs for inversion of C′ and C^α. The RF field for the pulses used in the FLOPSY-16 isotropic mixing sequence was 2.8 kHz and was applied for 170 ms. In the MOCCA-XY16 version pulses were given with an RF field of 12.0 kHz and several trials were done to evaluate the optimal delay Δ present in the MOCCA sequence (160–320 μs) and to optimise the mixing time (170–380 ms). To evaluate the performance of the MOCCA-XY16 isotropic mixing sequence with a lower RF field strength, additional experiments were acquired with an RF field of 5.4 kHz, with $\Delta = 260$ μs and with different mixing times (170 ms, 220 ms, 260 ms). Experiments were acquired with a relaxation delay of 1.3 s and with an acquisition time of 48 ms. The series of 2D C′–C′ correlation experiments were all run with the same SW (60 ppm), number of points (1,024 × 1,024) and scans (either 48 or 64). Spin echo and inversion recovery (both selective and non-selective) experiments were performed in the 1D mode on the carbonyl region to have a rough estimate on the overall relaxation properties of carbonyls.

Among the different spin state selection methods the IPAP method was selected to achieve virtual decoupling in the direct acquisition dimension. For each time increment in the indirect dimension two FIDs were separately stored, one for the anti-phase and one for the in-phase components. The two FIDs were then added and subtracted to separate the two multiplet components. These were then shifted to the centre of the original multiplet (by $J_{C'C\alpha}/2$ Hz) and again added to obtain a singlet (Bertini et al. 2004b; Bermel et al. 2006c).

Data were processed with the standard Bruker software (TopSpin 1.3). Simulations were run on a Linux-based PC with AMD Athlon processor using self-written code based on the program package SIMONE (Glaser and Drobny 1990). For the offset dependence of polarisation transfer 101 × 101 offsets in the range of −2,500 to 2,500 Hz were

used to calculate the normalised transfer efficiencies for FLOPSY-16, and two versions of the MOCCA-XY16 sequence as described in figure caption 2. For the calculations full supercycles were used and coupling constants were adjusted close to 1 Hz to assure that the condition $\tau_m = 1/(2\,J)$ is reached for the exact mixing times τ_m of 491.84, 497.02 and 497.04 ms for the FLOPSY-16 and the two MOCCA-XY16 sequences, respectively. No B_1-field inhomogeneity was taken into account. Contour plots were produced with a standard Matlab routine. The transverse weight w_t was calculated by integrating the normalised orientation vectors of the invariant trajectory at time steps corresponding to an effective flip angle of 5° for 64 offsets in the range between −2,500 and 2,500 Hz.

Theoretical framework

It has been shown previously that the MOCCA-XY16 multiple pulse sequence, originally designed for efficient Hartmann–Hahn-type transfer via residual dipolar couplings (Kramer et al. 2001), stores the magnetization mainly along the z-axis and therefore the relaxation processes that occur during the mixing time are dominated by longitudinal relaxation (Furrer et al. 2004). In proton homonuclear TOCSY experiments sensitivity gains of up to a factor three compared to conventional mixing sequences like FLOPSY-16 (Kadkhodaie et al. 1991) or DIPSI-2 (Shaka et al. 1988) could be obtained for long mixing times (Furrer et al. 2004).

The basic sequence consists of a simple building block Δ/2–180°–Δ/2 expanded in an XY16 supercycle (Gullion et al. 1990; Kramer et al. 2001). The same effective building block is also used in solid state experiments where it is called RFDR (Bennett et al. 1992; Sodickson et al. 1993) and in CPMG-type experiments (Gullion et al. 1990; Lizak et al. 1991; Skrynnikov et al. 2001) where it is used for spin locking and, e.g. the measurement of chemical/conformational exchange rates (Palmer et al. 1992; Mandel et al. 1996; Skrynnikov et al. 2001; Mulder et al. 2001). Depending on its application, it is important to adjust the delay Δ and the duration of the 180° pulse d correctly to obtain optimal performance of the multiple pulse sequence (Kramer et al. 2001; Furrer et al. 2004).

In the case of experiments correlating carbonyl nuclei, major issues are the efficient decoupling of the relatively large $^1J_{C'C}\alpha$ coupling to the C^α nuclei (52–55 Hz) and the significant relaxation loss of magnetization during the long mixing period needed as carbonyl–carbonyl coupling constants are small (Grzesiek and Bax 1997). The first issue, effective decoupling of C^α carbons, can best be obtained by adjusting the length d of the carbonyl 180° pulse in a way that C^α nuclei experience an effective n · 360° rotation. This is easily achieved using the well-known relation for square pulses $\omega_{eff} = \sqrt{\omega_{rf}^2 + \omega_{off}^2}$ with the RF-amplitude ω_{rf}, the offset ω_{off}, and the effective rotation frequency ω_{eff} at the given offset. Assuming that carbonyl nuclei are on-resonance and α-carbon nuclei resonate at the offset ω_{off}, the RF field necessary to achieve a flip angle of 180° (C′)/360° (C^α) implies the relation $2\omega_{rf} = \sqrt{\omega_{rf}^2 + \omega_{off}^2}$ or $\omega_{rf} = \omega_{off}/\sqrt{3}$. For the center of C′ and C^α frequencies at 176.8 ppm and 57.8 ppm, respectively, on a 16.4 T spectrometer, the offset is $\omega_{off} = 20.8$ kHz (119 ppm) and the corresponding RF-amplitude is $\omega_{rf} = 12.0$ kHz with a duration of the 180° pulse of $d = 41.6$ µs. The example is visualized in Fig. 1 using the effective flip angle $\varphi = d\omega_{eff}$ and the offset dependence of the inversion profile. If the RF-amplitude ω_{rf} is critical with respect to the applied energy, it is also possible to use the combination 180°(C′)/720°(C^α) with the relation $\omega_{rf} = \omega_{off}/\sqrt{15}$, resulting in $\omega_{rf} = 5.377$ kHz and

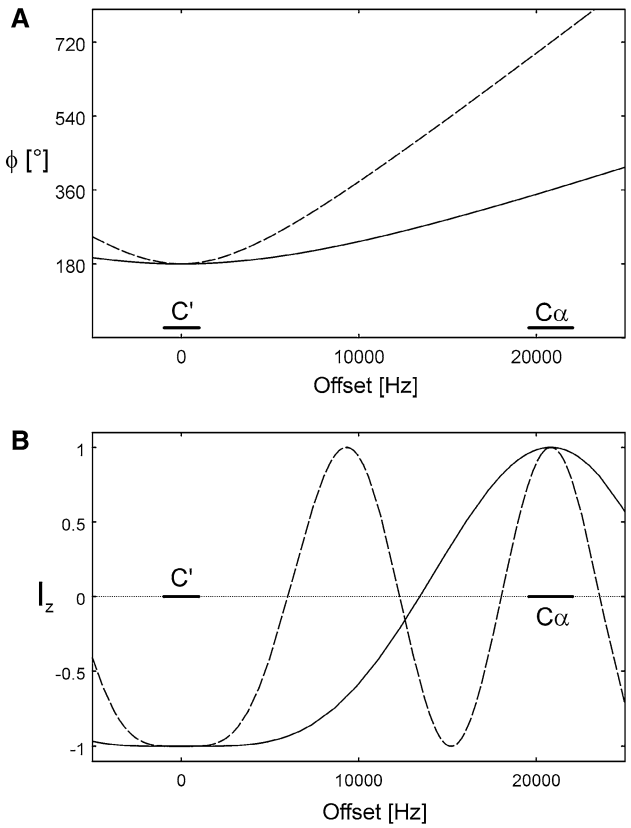

Fig. 1 Offset behaviour of inversion pulses designed for effective decoupling of C′ and C^α for a spectrometer frequency of 700 MHz. **a** Effective flip angle ϕ of a pulse with an RF-amplitude of 12,020 Hz and a duration of 41.6 µs (solid lines) and a pulse with 5,377 Hz RF-amplitude and 93 µs duration (dashed lines). **b** Corresponding inversion profiles for the two pulses, leading to a full inversion in the C′ region and to an effective 360° (solid line) or 720° (dashed line) rotation for C^α resonances

a duration of the 180° pulse of d = 93.0 µs for the given example at 16.4 T (Fig. 1, dashed lines).

The second issue, reducing losses due to relaxation, can be addressed as described in (Furrer et al. 2004). Assuming that the initial magnetisation is stored along z, the MOCCA-XY16 multiple pulse sequence only leads to transverse magnetization during the 180° pulses of length d, while it is kept longitudinal during the delays Δ. Therefore, the delay Δ has to be increased as much as possible without compromising polarisation transfer over the desired bandwidth to obtain a mixing sequence with optimal transfer properties. Assuming a desirable bandwidth for carbonyl–carbonyl transfer of approximately 10 ppm or 1,800 Hz at 16.4 T, simulations of the offset dependence of the polarization transfer lead to optimal delays Δ of 250–300 µs. The simulations were calculated assuming an ideal mixing time $1/(2J) \approx 500$ ms for a J-coupling close to 1 Hz in a two spin system as described in the Materials and Methods section and used previously for the characterisation of Hartmann–Hahn-type sequences (Glaser and Drobny 1990; Glaser and Quant 1996; Briand and Ernst 2008; Klages et al. 2007). In Fig. 2 the offset dependence of polarisation transfer for the FLOPSY-16 sequence, as previously applied in carbonyl–carbonyl experiments (Balayssac et al. 2006; Bermel et al. 2006b), is compared with two MOCCA-XY16 sequences with $\Delta/d = 2.8$, $d = 93$ µs, and $\Delta/d = 6.25$, $d = 41.6$ µs, respectively.

An approximate treatment of autorelaxation properties taking into account the offset-behaviour of the mixing sequence can be achieved with the invariant trajectory approach. (Glaser and Quant 1996; Griesinger and Ernst 1988; Bax 1989) The calculation of the transverse weight w_t and its application to the MOCCA-XY16 sequence has been described previously (Furrer et al. 2004). The method uses the motion of a normalised magnetisation vector $n(t) = [n_x(t), n_y(t), n_z(t)]$ under the action of a basis sequence after which the magnetisation vector returns to its initial orientation $n(\tau_b) = n(0)$. The effective autorelaxation rate ρ_{eff} of the invariant trajectory is then given by $\rho_{eff} = w_t \rho_t + w_l \rho_l$, with the transverse autorelaxation rate ρ_t and the longitudinal autorelaxation rate ρ_l and the transverse and longitudinal weights for the basic cycle with duration τ_b

$$w_t = \frac{1}{\tau_b} \int_0^{\tau_b} \{n_x(t)^2 + n_y(t)^2\}\, dt$$

and

$$w_l = \frac{1}{\tau_b} \int_0^{\tau_b} \{n_z(t)^2\}\, dt = 1 - w_t.$$

The offset dependence of w_t, which corresponds to the fraction of time during which the magnetisation is in the transverse plane during the mixing sequence, is shown in Fig. 3 for the FLOPSY-16 and the carbonyl–carbonyl transfer optimised MOCCA-XY16 variants. When approximating the longitudinal autorelaxation rate ρ_l by the relaxation rate R_1, as derived from inversion recovery experiments, and the transverse autorelaxation rate ρ_t by R_2, as derived from spin echo-type experiments, one can estimate an effective relaxation rate during a mixing sequence by $R_{eff} = (1 - w_t) R_1 + w_t R_2$. In this estimation, autorelaxation rates for zero quantum and double quantum coherences being present during TOCSY transfer are treated with R_1 and cross-relaxation rates are neglected. R_{eff} therefore can be considered to be a lower bound and the real value for the effective relaxation rate should be somewhat higher than R_{eff}. However, taking the invariant

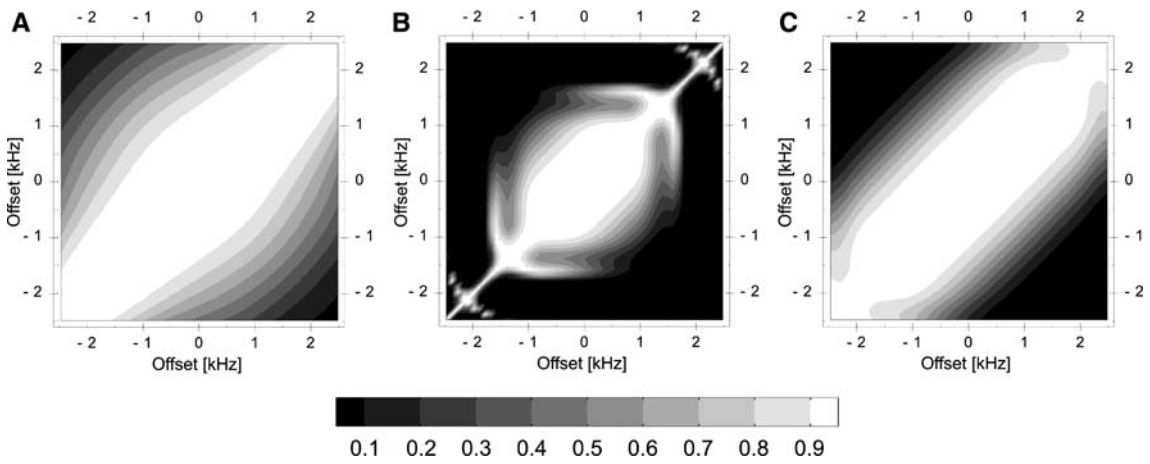

Fig. 2 Offset dependence of the polarisation transfer of three multiple pulse mixing sequences designed for effective carbonyl–carbonyl transfer in 2D experiments at a spectrometer frequency of 700 MHz. **a** The FLOPSY-16 sequence with an RF-amplitude of 2,777 Hz. **b** the MOCCA-XY16 sequence with a 180° pulse length of 93 µs and $\Delta/d = 2.8$. **c** the MOCCA-XY16 sequence with a 180° pulse length of 41.6 µs and $\Delta/d = 6.25$

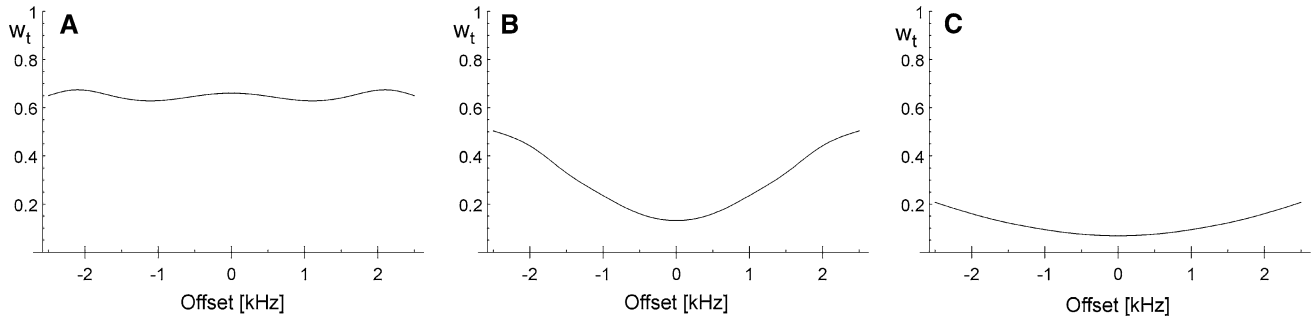

Fig. 3 Offset dependence of the transverse weight w_t from the invariant trajectory approach as derived in the main text for the three multiple pulse mixing sequences introduced in Fig. 2. **a** The FLOPSY-16 sequence with an RF-amplitude of 2,777 Hz. **b** the MOCCA-XY16 sequence with a 180° pulse length of 93 μs and $\Delta/d = 2.8$. **c** the MOCCA-XY16 sequence with a 180° pulse length of 41.6 μs and $\Delta/d = 6.25$

Table 1 Effective relaxation properties during various mixing sequences calculated for ubiquitin using the invariant trajectory approach as described in the text and experimental average relaxation rates of $R_1 = 0.76$ Hz and $R_2 = 13.0$ Hz

Sequence	R_{eff} [Hz]	T_{eff} [ms]	170 ms (%)	260 ms (%)
FLOPSY	8.70	115	22.75	10.4
MOCCA 720° ($\nu_{offs} = 0$)	2.48	400	67.8	52.4
MOCCA 720° ($\nu_{offs} = 1{,}000$ Hz)	3.95	253	51.1	36.8
MOCCA 360° ($\nu_{offs} = 0$)	1.7	590	75	64.3
MOCCA 360° ($\nu_{offs} = 1{,}000$ Hz)	2.08	480	70	58.2

Next to R_{eff} and $T_{eff} = 1/R_{eff}$, the effect of relaxation on the signal intensity for two mixing times with 100% magnetization at the beginning of isotropic mixing is given

trajectory-derived R_{eff} as a qualitative measure, it certainly gives a good trend for the relaxation rates during the isotropic mixing period. The effective relaxation rates and the resulting relative signal intensities for ubiquitin are summarized in Table 1 using experimentally measured values for the average R_1 and R_2 values of the carbonyls.

Results

The relative performance of the FLOPSY-16 and MOCCA-XY16 isotropic mixing sequences were compared by acquiring several experiments in the 2D mode on a uniformly ^{15}N, ^{13}C-labelled ubiquitin sample in which the kind of isotropic mixing scheme (FLOPSY-16 or MOCCA-XY16) and the delay Δ in the MOCCA-XY16 sequence were varied (160 μs, 240 μs, 320 μs) while leaving the overall mixing time and the 180° pulse fixed at durations of 170 ms and 41.6 μs, respectively. In Fig. 4, traces corresponding to one of the backbone correlations (65–66C′) in the four different experiments are reported as an example. The improved sensitivity can be clearly observed for the MOCCA-XY16 compared to the FLOPSY-16 mixing sequence. The sizeable improvement is obtained by changing the type of isotropic mixing sequence. In addition, the data are mildly dependent on the duration of the delay Δ and have a different behaviour for different cross peaks with maxima in the range of 240–330 μs. For cross peaks arising from side chain resonances, which are generally characterised by faster local mobility relative to backbone correlations, and thus by a different relaxation behaviour

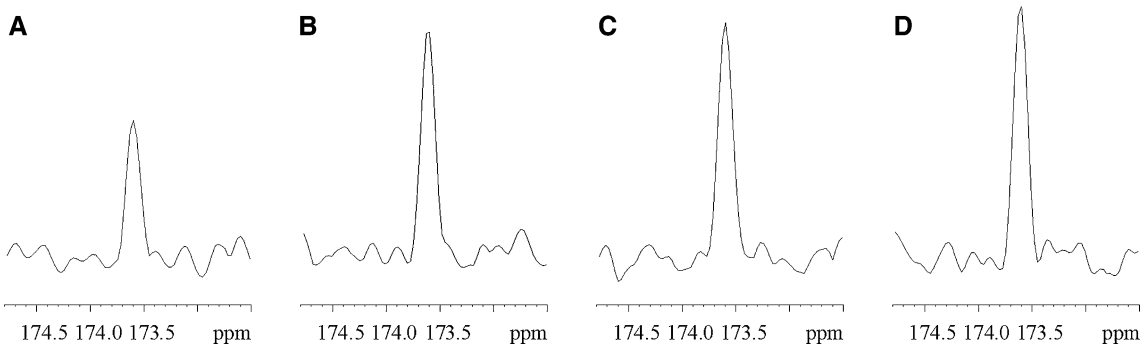

Fig. 4 Traces extracted from 2D C′, C′ correlation experiments acquired on ubiquitin employing two different kinds of isotropic mixing schemes (FLOPSY-16 (**a**) or MOCCA-XY16 (**b**–**d**)) and different delays Δ (160 μs (**b**), 240 μs (**c**), 320 μs (**d**)) in the latter. The mixing time in all cases was set to 170 ms. The peak shown corresponds to the correlation 65–66C′

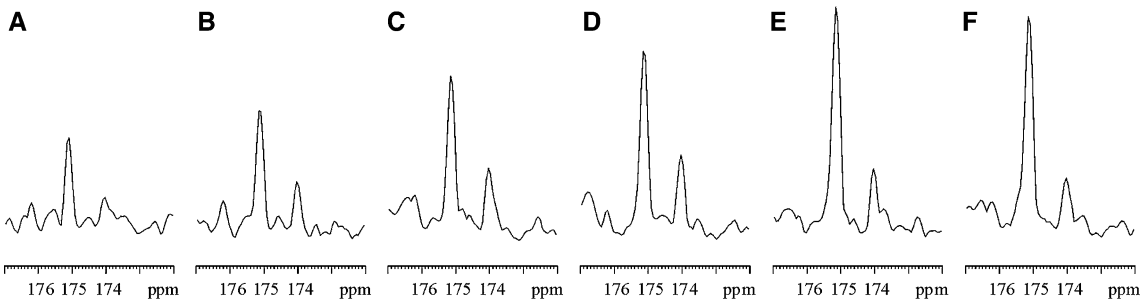

Fig. 5 Traces extracted from 2D C′, C′ correlation experiments acquired on ubiquitin employing the MOCCA-XY16 isotropic mixing scheme with $\Delta = 260$ µs and $d = 41.6$ µs, and with mixing times of 170 ms (**b**), 212 ms (**c**), 260 ms (**d**), 320 ms (**e**), and 380 ms (**f**). The equivalent experiment with a FLOPSY-16 mixing sequence (2,777 Hz RF-amplitude, 170 ms mixing time), is shown for comparison (**a**). The peaks shown correspond to the correlations 71C′–72N and 70C′–71N

with smaller transverse relaxation rates, the improvement upon change in the type of isotropic mixing sequence is much smaller and in many cases even negligible. This actually shows that the relaxation properties of the detected nuclear spins are the main factors affecting the improved performance of the MOCCA-XY16 isotropic mixing sequence for backbone C′–C′ correlations. The average sensitivity improvement obtained with the MOCCA-XY16 sequence corresponds to a factor 1.6 (up to factor 2.0 for individual signals) for cross peaks arising from backbone correlations.

Since the relaxation losses due to transverse relaxation are less dramatic in the MOCCA-XY16 isotropic mixing, one can think of increasing the duration of the isotropic mixing block. For this reason, an additional series of trial experiments was performed to evaluate the effect of an increase in the duration of the MOCCA-XY16 isotropic mixing time. Some traces extracted from the 2D experiments are shown as an example in Fig. 5 (71–72C′ and 70–71C′). In addition 2D regions for a subset of experiments are shown in Fig. 6 for which the increased number of correlations with the MOCCA-XY16 (170 and 260 ms mixing time) compared to the FLOPSY-16 isotropic mixing scheme (170 ms) can be observed. A gain in signal intensity of cross peaks can be observed up to a mixing time of approximately 260 ms while the use of longer mixing periods on average do not improve the spectrum further. This behaviour can be rationalised by the expected coherence transfer function, which, for three linearly and equally coupled spins, should have a maximum at $1/(4J)$ (Eaton et al. 1990; Schedletzky and Glaser 1996; Luy et al. 1999; Luy and Glaser 2001). For a small $^3J_{C'-C'}$ coupling of 1 Hz, the maximum transfer would then be at 250 ms under ideal Hartmann–Hahn conditions. Owing to the effective relaxation of carbonyls, the damped coherence transfer function with its maximum at approximately 260 ms is indicative of transfer via couplings of sizes $^3J_{C'-C'} < 1$ Hz. With the additional advantage of increased mixing times the overall gain in sensitivity is improved up to a factor 2.3.

Isotropic mixing periods of several hundred milliseconds at intermediate RF-amplitudes are very demanding for a high resolution probehead. The root mean square RF-power applied with the 180°(C′)/360°(C^{α}) solution on a

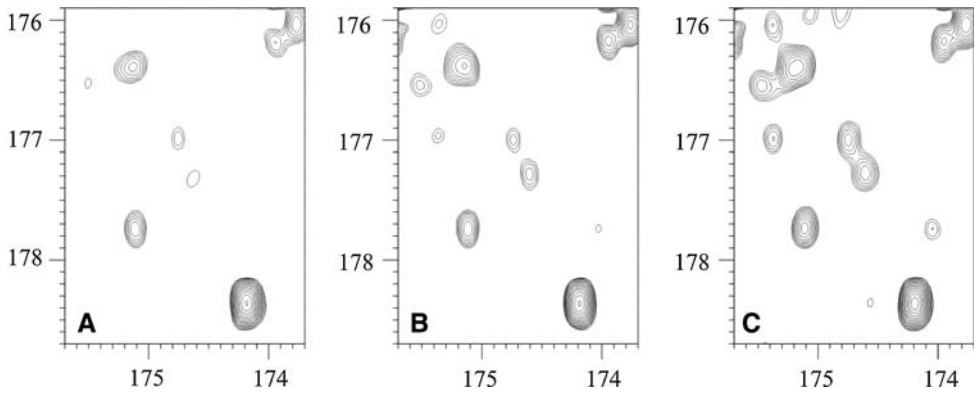

Fig. 6 Selected 2D-region of the C′, C′ experiments acquired with different isotropic mixing schemes and mixing times; **a** FLOPSY-16 (170 ms mixing time, 2777 Hz RF-amplitude), **b** MOCCA-XY16 (170 ms mixing time, $\Delta = 260$ µs and $d = 41.6$ µs) and **c**) MOCCA-XY16 (260 ms mixing time, $\Delta = 260$ µs and $d = 41.6$ µs). The most intense correlation in the 2D plots at 174.2 ppm is due to a side chain carbonyl carbon and expectedly does not change intensity in the three cases

16.4 T magnet corresponds to a constant amplitude pulse sequence of 4,464 Hz compared to the FLOPSY-16 variant with only 2,777 Hz. Since the energy applied to the probehead is proportional to the square of the RF-amplitude, the factor 2.6 increase of the total energy applied to the sample can easily exceed the specifications of a given probehead. Since the applied RF-amplitudes also must be scaled with the field strength, the probehead requirements are even more stringent at stronger magnetic fields. Therefore, an alternative solution that exploits pulses with lower power, still with the wanted properties (inversion on carbonyls signals, on-resonance, and $n \cdot 360°$ off-resonance on C^{α}s) may be needed. For this reason, we also tested the behaviour of the lower power MOCCA-XY16 isotropic mixing sequence. It exploits $180°(C')/720°(C^{\alpha})$ pulses with optimised delays $\Delta \approx 260$ µs which results in a root mean square RF-power corresponding to a constant amplitude pulse sequence of 2,760 Hz. The observed signal intensities decrease compared to the high power $180°(C')/360°(C^{\alpha})$ case in agreement with what was expected, but still give an increase in the intensities of cross peaks compared to the FLOPSY-16 case (with overall improvement factors up to 2 for 260 ms mixing time).

Discussion

Protonless NMR spectroscopy has proven in many examples to provide excellent tools for special classes of proteins like paramagnetic, fully deuterated, or unfolded proteins. In particular, the experiments that exploit carbonyl direct detection are very useful for the assignment of otherwise poorly resolved molecules (Bermel et al. 2006b). One of the experiments to detect sequence specific correlations is based on the carbonyl–carbonyl isotropic mixing scheme. The isotropic mixing period in such experiments is quite long, typically exceeding 150 ms, and mixing sequences with reduced relaxation losses like the specifically adapted MOCCA-XY16 scheme presented here will significantly enhance the applicability of the experiment.

The favourable relaxation properties of the MOCCA-XY16 isotropic mixing sequence improve markedly the experimental performance, particularly in those cases where a long mixing time is necessary to allow for evolution of fairly small 3-bond scalar coupling constants. For this reason, thanks to the relaxation optimized building block, the mixing time can also be further increased in order to allow for more evolution of the small couplings, as relaxation losses are considerably reduced.

A quick estimate of the transverse and longitudinal relaxation rates of carbonyls of ubiquitin, as evaluated through 1D experiments using the whole envelope of carbonyl backbone signals ($R_1 = 0.76\ s^{-1}$ and $R_2 = 13\ s^{-1}$) can be used to give an upper estimate for the expected gain based on the different effective relaxation rates during the two different isotropic mixing schemes, as explained in the previous section. As reported in Table 1, this upper estimate would lead to a relaxation-based increase up to a factor of about 3. Depending on the selected correlation in the 2D maps, we experimentally observed gains ranging from no gain up to a factor of 2 improvements. The distribution of this increase can be attributed to three factors: first, the mixing time dependence of the coherence transfer depends on all spins coupled within a spin system and can be quite complicated for three or more coupled spins (Eaton et al. 1990; Schedletzky and Glaser 1996; Luy et al. 1999; Luy and Glaser 2001); second, the slight variation of transfer efficiency with the offset can lead to varying signal intensities, and third, the different relaxation behaviour of different backbone nuclear spins must be considered when comparing individual signals (the rates used for the simulations were measured on the envelope of backbone signals and do not account for internal variations). An examination of correlations with backbone carbonyls with known lower relaxation rates proves that the observed improvements are mainly caused by different effective relaxation rates during the isotropic mixing sequences.

The relaxation of carbonyls is mainly determined by the strong chemical shift anisotropy which scales quadratic with the static magnetic field. Especially at higher magnetic field strengths the sensitivity improvements due to the relaxation enhanced MOCCA-XY16 scheme can therefore be expected to further increase.

The optimisation of the MOCCA-XY16 isotropic mixing sequence was performed here for a spectrometer operating at 16.4 T. Concerning the MOCCA-XY16 building block, the effective relaxation rate during mixing is only determined by the ratio Δ/d, which, here, is 6.25 for the high power $180°(C')/360°(C^{\alpha})$ and 2.8 for the lower power $180°(C')/720°(C^{\alpha})$ variant, respectively. When applying the MOCCA-XY16 mixing scheme to correlate backbone carbonyls at different magnetic field strengths, the chemical shift-difference of C' and C^{α} also scales with the magnetic field and the corresponding pulse length d in the mixing scheme has to be adjusted. For the $180°(C')/360°(C^{\alpha})$ case the pulse length in µs is given by $d = 29{,}120/\nu_{1H}$ and the corresponding RF-amplitude in Hz by $\nu_{rf} = 17.171 \cdot \nu_{1H}$ with the ^1H spectrometer frequency ν_{1H} in MHz. The corresponding formulae for the $180°(C')/720°(C^{\alpha})$ case are $d = 65{,}100/\nu_{1H}$ and $\nu_{rf} = 7.681 \cdot \nu_{1H}$, respectively. The optimum MOCCA-XY16 delay in all cases is given by $\Delta \approx 182{,}200/\nu_{1H}$. Example values for three spectrometer frequencies are given in Table 2.

Especially at high magnetic field strengths the application of the high power $180°(C')/360°(C^{\alpha})$ version of the MOCCA-XY16 sequence for extended mixing times

Table 2 Parameters for the MOCCA-XY16 mixing scheme optimised for C′, C′-correlation experiments at various magnetic field strengths

Proton Frequency [MHz]	MOCCA-XY16 with 180° (C′)/360° (C^{α}) pulses	MOCCA-XY16 with 180° (C′)/720° (C^{α}) pulses
1,000	d = 29.1 μs; Δ = 182.2 μs	d = 65.1 μs; Δ = 182.2 μs
800	d = 36.4 μs; Δ = 227.7 μs	d = 81.4 μs; Δ = 227.7 μs
600	d = 48.5 μs; Δ = 303.6 μs	d = 108.5 μs; Δ = 303.6 μs

See text for 16.4 T (700 MHz) spectrometer data and the discussion section for a general formula

should be planned with care. When in doubt whether a given probehead can bear the induced RF-energy, please contact the manufacturer for specifications. It should be noted that probeheads designed for direct ^{13}C-detection are generally less affected by the applied RF-energy than corresponding probeheads optimized for ^{1}H direct detection. For most probeheads with the latter design the lower power 180°(C′)/720°(C^{α}) version of the MOCCA-XY16 scheme seems more appropriate.

A final comment is due on the fact that this specific isotropic mixing sequence (MOCCA-XY16) actually leaves the ^{13}C magnetization for a large part of the mixing time along the z-axis, free to evolve. These are conditions in which also nuclear Overhauser effects (and dipolar couplings) do evolve and so one should also consider which impact this will have on the final results. Due to the frequent 180° selective C′ pulses the evolution of carbon–carbon NOEs other than those involving two nuclei affected by these pulses (carbonyls) will actually be quenched (Vincent et al. 1996). The NOEs between carbonyls are expected to be quite small effects, especially in intrinsically unstructured proteins, so that they should not contribute to the observed signals. The combined evolution of NOE and scalar transfer can instead be very advantageous in other cases, such as the C–C transfer between aliphatic (or aromatic) carbon nuclei and may contribute to additional sensitivity in large systems, where it has been proven that the NOESY effect can be quite large and gives informative spectra in short time (Bertini et al. 2004c; Matzapetakis et al. 2007; Bermel et al. 2007).

Conclusion

In summary, we have shown that an adapted version of the MOCCA-XY16 mixing sequence allows a significant reduction of relaxation losses during the isotropic mixing period in experiments that exploit carbonyl–carbonyl transfer mediated by the small ^{3}J scalar coupling. A gain in sensitivity of up to two compared to equivalent experiments employing FLOPSY-16 mixing periods is achieved. With this significant increase of the signal-to-noise-ratio the improved version can be expected to considerably help in the assignment process, especially for unfolded proteins where carbonyl nuclei have favourable relaxation properties and retain high chemical shift dispersion.

Acknowledgments This work has been supported in part by the EC contracts EU-NMR n° 026145 (TA and JRA) and SPINE II n° 031220 and by Ente Cassa di Risparmio di Firenze. S. J. G. and B. L. thank the Fonds der Chemischen Industrie and the Deutsche Forschungsgemeinschaft for financial support (GL 203/6–1; Emmy Noether and Heisenberg fellowships LU 835/1–4 and LU 835/2–1). B. L. thanks the Center for Integrated Protein Science Munich (CIPSM) for financial support. Prof. Ivano Bertini is gratefully acknowledged for stimulating discussions.

References

Arnesano F, Banci L, Bertini I, Felli IC, Luchinat C, Thompsett AR (2003) A strategy for the NMR characterization of type II copper(II) proteins: the case of the copper trafficking protein CopC from *Pseudomonas syringae*. J Am Chem Soc 125:7200–7208

Babini E, Bertini I, Capozzi F, Felli IC, Lelli M, Luchinat C (2004) Direct carbon detection in paramagnetic metalloproteins to further exploit pseudocontact shift restraints. J Am Chem Soc 126:10496–10497

Balayssac S, Jiménez B, Piccioli M (2006) ^{13}C Direct Detected COCO-TOCSY: a tool for sequence specific assignment and structure determination in *protonless* NMR experiments. J Magn Reson 182:325–329

Bax A (1989) Homonuclear magnetization transfer experiments using isotropic and nonisotropic mixing schemes. Israel J Chem 28:309–317

Bennett AE, Griffin RG, Ok JH, Vega S (1992) Chemical shift correlation spectroscopy in rotating solids: radio frequency-driven dipolar recoupling and longitudinal exchange. J Chem Phys 96:8624–8627

Bermel W, Bertini I, Felli IC, Kümmerle R, Pierattelli R (2003) ^{13}C direct detection experiments on the paramagnetic oxidized monomeric copper, zinc superoxide dismutase. J Am Chem Soc 125:16423–16429

Bermel W, Bertini I, Duma L, Emsley L, Felli IC, Pierattelli R, Vasos PR (2005a) Complete assignment of heteronuclear protein resonances by *protonless* NMR spectroscopy. Angew Chem Int Ed 44:3089–3092

Bermel W, Bertini I, Felli IC, Pierattelli R, Vasos PR (2005b) A selective experiment for the sequential protein backbone assignment from 3D heteronuclear spectra. J Magn Reson 172:324–328

Bermel W, Bertini I, Felli IC, Kümmerle R, Pierattelli R (2006a) Novel ^{13}C direct detection experiments, including extension to the third dimension, to perform the complete assignment of proteins. J Magn Reson 178:56–64

Bermel W, Bertini I, Felli IC, Lee Y-M, Luchinat C, Pierattelli R (2006b) *Protonless* NMR experiments for sequence-specific assignment of backbone nuclei in unfolded proteins. J Am Chem Soc 128:3918–3919

Bermel W, Bertini I, Felli IC, Piccioli M, Pierattelli R (2006c) ^{13}C-detected *protonless* NMR spectroscopy of proteins in solution. Progr NMR Spectrosc 48:25–45

Bermel W, Felli IC, Matzapetakis M, Pierattelli R, Theil EC, Turano P (2007) A method for C^{α} direct-detection in *protonless* NMR. J Magn Reson 188:301–310

Bermel W, Bertini I, Csizmok V, Felli IC, Pierattelli R and Tompa P (accepted) H-start for exclusively heteronuclear NMR spectroscopy: the case of intrinsically disordered proteins

Bertini I, Lee Y-M, Luchinat C, Piccioli M, Poggi L (2001) Locating the metal ion in calcium-binding proteins by using cerium(III) as a probe. ChemBioChem 2:550–558

Bertini I, Duma L, Felli IC, Fey M, Luchinat C, Pierattelli R, Vasos PR (2004a) A heteronuclear direct detection NMR experiment for protein backbone assignment. Angew Chem Int Ed 43:2257–2259

Bertini I, Felli IC, Kümmerle R, Luchinat C, Pierattelli R (2004b) ^{13}C–^{13}C NOESY: a constructive use of ^{13}C–^{13}C spin-diffusion. J Biomol NMR 30:245–251

Bertini I, Felli IC, Kümmerle R, Moskau D, Pierattelli R (2004c) ^{13}C–^{13}C NOESY: an attractive alternative to study large macromolecules. J Am Chem Soc 126:464–465

Bertini I, Felli IC, Luchinat C, Parigi G, Pierattelli R (2007) Towards a protocol for solution structure determination of copper(II) proteins: the case of Cu(II)Zn(II) superoxide dismutase. ChemBioChem 8:1422–1429

Boehlen J-M, Bodenhausen G (1993) Experimental aspects of chirp NMR spectroscopy. J Magn Reson Ser A 102:293–301

Braunschweiler L, Ernst RR (1983) Coherence transfer by isotropic mixing: application to proton correlation spectroscopy. J Magn Reson 53:521–528

Breitmaier E, Jung G, Voelters W (1970) Pulse Fourier transform ^{13}C-NMR spectroscopy, principles and applications. Angew Chem Int Ed Engl 10:673–686

Briand J, Ernst RR (2008) Computer-optimized homonuclear TOCSY experiments with suppression of cross relaxation. Chem Phys Lett 185:276

Caillet-Saguy C, Delepierre M, Lecroisey A, Bertini I, Piccioli M, Turano P (2006) Direct detected ^{13}C NMR to investigate the Iron(III) hemophore HasA. J Am Chem Soc 128:150–158

Eaton HL, Fesik SW, Glaser SJ, Drobny GB (1990) Time dependence of ^{13}C–^{13}C magnetization transfer in isotropic mixing experiments involving amino acid spin systems. J Magn Reson 90:452–463

Eletsky A, Moreira O, Kovacs H, Pervushin K (2003) A novel strategy for the assignment of side-chain resonances in completely deuterated large proteins using (13)C spectroscopy. J Biomol NMR 26:167–179

Emsley L, Bodenhausen G (1990) Gaussian pulse cascades: new analytical functions for rectangular selective inversion and in-phase excitation in NMR. Chem Phys Lett 165:469–476

Farès C, Amata I, Carlomagno T (2007) ^{13}C-detection in RNA bases: revealing structure–chemical shift relationships. J Am Chem Soc 129:15814–15823

Fiala R, Sklenar V (2007) ^{13}C-detected NMR experiments for measuring chemical shifts and coupling constants in nucleic acid bases. J Biomol NMR 39:152–163

Furrer J, Kramer F, Marino JP, Glaser SJ, Luy B (2004) Homonuclear Hartmann–Hahn transfer with reduced relaxation losses by use of the MOCCA-XY16 multiple pulse seqeunce. J Magn Reson 166:39–46

Glaser SJ, Drobny GP (1990) Assessment and optimization of pulse sequences for homonuclear isotropic mixing. In: Warren WS (ed) Advances in magnetic resonance, vol 14. Academic Press, New York, pp 35–58

Glaser SJ, Quant JJ (1996) Homonuclear and heteronuclear Hartmann–Hahn transfer in isotropic liquids. In: Warren WS (ed) Advances in magnetic and optical resonance, vol 19. Academic Press, New York, pp 59–252

Griesinger C, Ernst RR (1988) Cross relaxation in time dependent nuclear spin systems—invariant trajectory approach. Chem Phys Lett 152:239–247

Grzesiek S, Bax A (1997) A three-dimensional NMR experiment with improved sensitivity for carbonyl–carbonyl *J* correlation in proteins. J Biomol NMR 9:207–211

Gullion T, Baker DB, Conradi MS (1990) New, compensated Carr–Purcell sequences. J Magn Reson 89:479–484

Hu K, Vögeli B, Clore GM (2007) Spin-state selective carbon-detected HNCO with TROSY optimization in all dimensions and double echo–antiecho sensitivity enhancement in both indirect dimensions. J Am Chem Soc 129:5484–5491

Kadkhodaie M, Rivas O, Tan M, Mohebbi A, Shaka AJ (1991) Broadband homonuclear cross polarization using flip–flop spectroscopy. J Magn Reson 91:437–443

Klages J, Kessler H, Glaser SJ, Luy B (2007) J-ONLY-TOCSY: efficient suppression of RDC-induced transfer in homonuclear TOCSY experiments using JESTER-1-derived multiple pulse sequences. J Magn Reson 189:217–227

Kolczak U, Salgado J, Siegal G, Saraste M, Canters GW (1999) Paramagnetic NMR studies of blue and purple copper proteins. Biospectroscopy 5:S19–S32

Kostic M, Pochapsky SS, Pochapsky TC (2002) Rapid recycle ^{13}C, ^{15}N and ^{13}C,^{13}C heteronuclear and homonuclear multiple quantum coherence detection for resonance assignments in paramagnetic proteins: example of Ni^{2+}-containing acireductone dioxygenase. J Am Chem Soc 124:9054–9055

Kovacs H, Moskau D, Spraul M (2005) Cryogenically cooled probes—a leap in NMR technology. Progr NMR Spectrosc 46:131–155

Kramer F, Peti W, Griesinger C, Glaser SJ (2001) Optimized homonuclear Carr–Purcell-type dipolar mixing sequences. J Magn Reson 149:58–66

Liu A, Riek R, Wider G, Von Schroetter C, Zahn R, Wüthrich K (2000) NMR experiments for resonance assignments of ^{13}C, ^{15}N doubly-labeled flexible polypeptides: application to the human prion protein hPrP(23-230). J Biomol NMR 16:127–138

Lizak MJ, Gullion T, Conradi MS (1991) Measurements of like-spin dipole couplings. J Magn Reson 91:254–260

Luy B, Glaser SJ (2001) Superposition of scalar and residual dipolar couplings: analytical transfer functions for three spins 1/2 under cylindrical mixing conditions. J Magn Reson 148:169–181

Luy B, Schedletzky O, Glaser SJ (1999) Analytical polarization transfer functions for four coupled spins 12 under isotropic mixing conditions. J Magn Reson 138:19–27

Machonkin TE, Westler WM, Markley JL (2002) ^{13}C–^{13}C 2D NMR: a novel strategy for the study of paramagnetic proteins with slow electronic relaxation times. J Am Chem Soc 124:3204–3205

Mandel AM, Akke M, Palmer AG (1996) Dynamics of ribonuclease H: temperature dependence of motions on multiple time scales. Biochemistry 35:16009–16023

Matzapetakis M, Turano P, Theil EC, Bertini I (2007) ^{13}C–^{13}C NOESY spectra of a 480 kDa protein: solution NMR of ferritin. J Biomol NMR 38:237–242

Mulder FAA, Skrynnikov NR, Hon B, Dahlquist FW, Kay LE (2001) Measurement of slow (μs–ms) time scale dynamics in protein side chains by N-15 relaxation dispersion NMR spectroscopy: application to Asn and Gln residues in a cavity mutant of T4 lysozyme. J Am Chem Soc 123:967–975

Oh B-H, Westler WM, Darba P, Markley JL (1988) Protein carbon-13 spin systems by a single two-dimensional nuclear magnetic resonance experiment. Science 240:908–911

Palmer AGIII, Skelton NJ, Chazin WJ, Wright PE, Rance M (1992) Suppression of the effects of cross-correlation between dipolar

and anisotropic chemical shift relaxation mechanisms in the measurement of spin–spin relaxation rates. Mol Phys 75: 699–711

Schedletzky O, Glaser SJ (1996) Analytical coherence-transfer functions for the general AMX spin system under isotropic mixing. J Magn Reson Ser A 123:174–180

Shaka AJ, Keeler J, Freeman R (1983) Computer-optimized decoupling scheme for wideband applications and low-level operation. J Magn Reson 53:313–340

Shaka AJ, Barker PB, Freeman R (1985) Evaluation of a new broadband decoupling sequence: WALTZ-16. J Magn Reson 64:547–552

Shaka AJ, Lee CJ, Pines A (1988) Iterative schemes for bilinear operators: application to spin decoupling. J Magn Reson 77: 274–293

Skrynnikov NR, Mulder FAA, Hon B, Dahlquist FW, Kay LE (2001) Probing slow time scale dynamics at methyl-containing side chains in proteins by relaxation dispersion NMR measurements: application to methionine residues in a cavity mutant of T4 lysozyme. J Am Chem Soc 123:4556–4566

Sodickson DK, Levitt MH, Vega S, Griffin RG (1993) Broad-band dipolar recoupling in the nuclear magnetic resonance of rotating solids. J Chem Phys 98:6742–6748

Vincent SJF, Zwahlen C, Bodenhausen G (1996) Suppression of spin diffusion in selected frequency bands of nuclear Overhauser spectra. J Biomol NMR 7:169–172

Vögeli B, Kovacs H, Pervushin K (2004) Measurements of side chain ^{13}C–^{13}C residual dipolar coupling in uniformly deuterated proteins. J Am Chem Soc 126:2414–2420